International Journal of Remote Sensing
Vol. 27, No. 16, 20 August 2006, 3455–3471

Assessing spatio-temporal variations in plant phenology using Fourier analysis on NDVI time series: results from a dry savannah environment in Namibia

H. WAGENSEIL* and C. SAMIMI
Institute of Geography, Friedrich-Alexander-Universität Erlangen-Nürnberg, Kochstrasse 4/4, D-91054 Erlangen, Germany

(*Received 27 February 2005; in final form 10 February 2006*)

Time series of Normalized Difference Vegetation Index (NDVI) from the Advanced Very High Resolution Radiometer (AVHRR) were used to capture plant phenology in Etosha National Park, a dry savannah environment in Namibia. Data from two consecutive growing periods with different precipitation conditions were included to study impacts of inter-seasonal rainfall variations on a highly water-limited ecosystem. Additionally, a contemporary reference map with four major vegetation units was used to compare phenology between plant formations. Phenological attributes were acquired for both seasons using Fourier analysis. Parameters were calculated for the entire study area and further stratified with respect to the mapping units of the reference. Vegetation growth was found to vary significantly between the two periods in accordance with available rainfall data. Additionally, separability of vegetation entities based on Fourier parameters was weak due to within-class scattering and was commonly outranged by inter-seasonal variations. Finally, discrimination of cover types was tested by combining selected Fourier parameters in a clustering procedure. Spatial class distribution was compared to the reference statistically and only a moderate correspondence was discovered. We conclude that Fourier-based NDVI attributes are limited for cover-type discrimination across space and time, as they only quantify certain aspects of plant phenology and seem to be largely altered by the actual rainfall situation.

1. Introduction

In many regions of the world, pressure on natural resources is steadily increasing due to rapid population growth. This especially applies to Africa, where tropical savannahs cover about 40% of the land surface and are used by a large part of the population for agriculture (Scholes and Walker 1993, Schultz 2000). Thus, land degradation is nowadays a widespread problem throughout the entire continent (World Bank Group 2004). In dry savannahs, where livestock farming is prevalent, degradation from overgrazing is often expressed by decreasing vegetation coverage (Pickup and Chewings 1994), bush encroachment (Higgins *et al.* 1999, Roques *et al.* 2001) or changes in community composition (Scholes and Walker 1993), and reduced rain-use efficiency (Diouf and Lambin 2001, Li *et al.* 2004). These problems not only affect farmlands, but also national parks, especially if the game population

*Corresponding author. Email: hwagense@geographie.uni-erlangen.de

International Journal of Remote Sensing
ISSN 0143-1161 print/ISSN 1366-5901 online
http://www.tandf.co.uk/journals
DOI: 10.1080/01431160600639743

density is high and fences bound the natural mobility of the animals (Beugler-Bell 1996).

Although separating human-induced degradation from natural variability often remains a challenge (Pickup and Chewings 1994, Diouf and Lambin 2001), the above findings highlight that continuous vegetation mapping is becoming increasingly important for monitoring changes and identifying affected areas (Justice *et al.* 1986, Malingreau *et al.* 1989, Al-Bakri and Taylor 2003, Li *et al.* 2004). As ground based surveys are rarely economically feasible, remote sensing often remains the only useful tool (Pickup and Chewings 1994, Du Plessis 1999).

1.1 *Background*

Studying and mapping vegetation from satellite data are widely performed by use of the Normalized Difference Vegetation Index (NDVI). This index accounts for the converse reflectance properties of green vegetation in the near infrared (NIR) and red (R) parts of the solar spectrum and is defined as:

$$\mathrm{NDVI} = (\mathrm{NIR} - \mathrm{R})/(\mathrm{NIR} + \mathrm{R}) \tag{1}$$

NDVI is accepted for capturing essential vegetation parameters such as green leaf biomass, leaf area index, percent green cover, green biomass production and annual net primary production (Justice and Hiernaux 1986, Diallo *et al.* 1991, Prince 1991, Carlson and Ripley 1997, Diouf and Lambin 2001, Sannier *et al.* 2002).

Additionally, time series of NDVI reflect the seasonal dynamics of vegetation with respect to photosynthetic activity. Based on phenological differences, major vegetation formations have been mapped successfully at different scales (Justice *et al.* 1986, Kremer and Running 1993, Defries *et al.* 1995, Moulin *et al.* 1997, Azzali and Menenti 2000). Typically, this is performed by deriving a number of metrics from multitemporal NDVI data such as maximum, minimum or length of the growing season (Reed *et al.* 1994, Defries *et al.* 1995), which are then grouped by some clustering algorithm to produce map units with similar phenological characteristics. Additionally, statistical approaches have been used to derive NDVI parameters, amongst which Fourier analysis has been paid much attention (Azzali and Menenti 2000, Eiden 2000, Jakubauskas *et al.* 2001, Moody and Johnson 2001).

In dry savannahs, however, inter-seasonal variations in local rainfall complicate phenology-based mapping approaches, as plant growth is water-limited and thus NDVI is also strongly related to actual precipitation (e.g. Davenport and Nicholson 1993, Richard and Poccard 1998, Du Plessis 1999, Li *et al.* 2004, Xiao and Moody 2004). This provokes phenological patterns to vary not only between plant communities, but also between seasons. Mapping approaches based on temporal metrics are thus mostly applied by averaging NDVI time series for multiple seasons to minimize rainfall-induced variations (Sannier *et al.* 1996, Eiden 2000, Moody and Johnson 2001).

1.2 *Study objectives*

Despite the substantial control of rainfall on NDVI, there is evidence that certain temporal growth patterns remain distinguishable for vegetation units at least on a broad scale, even in water-controlled environments (e.g. Nicholson and Farrar 1994). Additionally, inter-seasonal variations of phenological metrics from NDVI time series have not yet been studied in very much detail, although there is a high demand on parameters, which are suitable to describe vegetation distribution continuously, as well as on methods to derive these metrics objectively.

For this paper, we accept Fourier analysis to be an established method to derive phenological metrics (mean, amplitude and phase) from NDVI time series, which is in accordance with a number of recently published papers (Azzali and Menenti 2000, Jakubauskas *et al.* 2001, Moody and Johnson 2001). Our study site is Etosha National Park (ENP) in northern Namibia (figure 1), a semi-arid area with high rainfall variability (Mendelsohn *et al.* 2002). We compared spatial patterns of these metrics for two selected and consecutive growing periods, which showed pronounced differences in rainfall distribution. A contemporary vegetation map of ENP serves as a reference to establish relationships between the metrics and major vegetation units. Restricting our procedure to only two seasons allows us to relate spatio-temporal changes of NDVI metrics to variations in rainfall only, as major changes in vegetation distribution can be neglected for this short period. If differences in the metrics are more significant between vegetation entities than between the different seasons, then the approach can easily be extended to test applicability on a multi-seasonal scale.

2. Materials and methods

2.1 *Regional settings*

Etosha National Park (ENP) is located in northern Namibia between 18°30′ S–19°33′ S and 14°24′ E–17°08′ E covering 22 700 km^2 (Mendelsohn *et al.* 2002, figure 1). It is completely fenced, has a dense game population and is one of the biggest wildlife reserves in the world. Apart from the south-western corner, the park is situated on the continental plateau with an elevation of 1073 m to 1270 m a.s.l. (Beugler-Bell 1996). The Etosha pan, a saline desert covering one fifth of the total area, is the most obvious landscape feature within the park.

The climate of northern Namibia is semi-arid with a rainy season in summer (October to April) caused by isolated convective storms. On a long-term average, there is an east–west rainfall gradient within ENP from 450 mm (Namutoni) to 250 mm (Otjovasandu) with a seasonal maximum usually around February (Beugler-Bell 1996, Mendelsohn *et al.* 2002). However, variability is very high across space and time as suggested by the coefficient of variation, which increases from approximately 30% in the east up to 50% in the west (Mendelsohn *et al.* 2002,

Figure 1. Location of the study area in northern Namibia.

Sannier *et al.* 2002). Thus, for any location, rainfall amounts vary largely within a given season and between seasons.

The vegetation largely consists of shrub and tree savannah (figure 2). *Colophospermum mopane* is the dominant species in both woody layers, but can often be found in combination with *Combretum apiculatum, Terminalia prunioides* and *Dichrostachys cinerea*. Further *Catophractes alexandri, Acacia mellifera* and *Acacia nebrownii* are important components of the shrub layer (Le Roux *et al.* 1988). Especially around the pan, small plains of grassland and steppe occur, which are important grazing sites for game (Beugler-Bell 1996, Sannier *et al.* 2002).

2.2 *Reference data*

The only available reference map showing the distribution of four major vegetation units was created in 1993 from a supervised Landsat Thematic Mapper (TM) classification (figure 2). This reference was validated against ground surveys and determined to have an overall accuracy of more than 89% for the units bare soil, grassland, shrub savannah and tree savannah (Sannier *et al.* 1996, Taylor *et al.* 1996). The original map was achieved by the Etosha Ecological Institute (EEI), a research institute based inside ENP, at a spatial resolution of 25 m × 25 m. A 45 × 45 modal filter followed by a nearest neighbour resampling were applied to degrade the resolution down to approximately 1 km × 1 km.

Rainfall data for selected stations inside ENP were additionally provided by the EEI and were explored to select growing seasons temporally close to the reference, but with different precipitation conditions. The limited data availability did not allow any quantitative and objective measures to be used, so the selection is based on qualitative data inspection only. However, we assume the rainfall conditions for 1993/1994 (figure 3(*a*)) and 1994/1995 (figure 3(*b*)) to be dissimilar enough to test our approach.

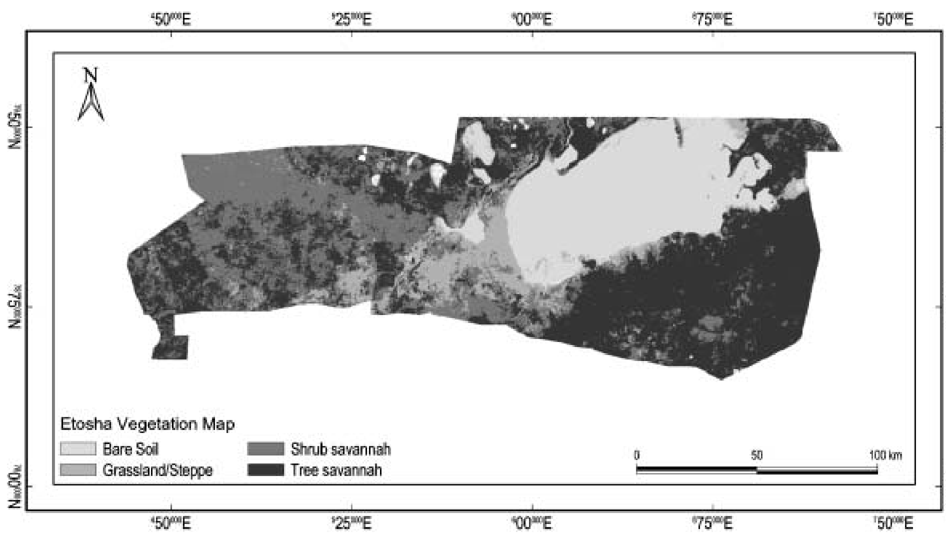

Figure 2. Distribution of major vegetation units across Etosha National Park (source: EEI, see also Sannier *et al.* 1996, Taylor *et al.* 1996).

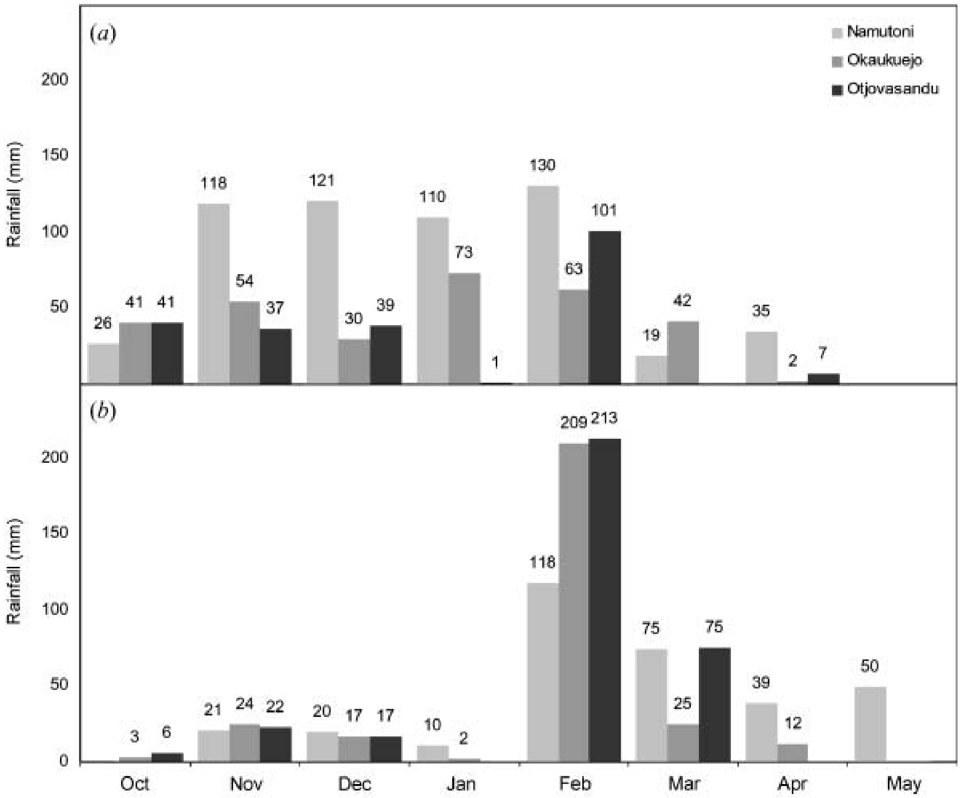

Figure 3. Rainfall (mm) recorded at selected stations in ENP during (*a*) 1993/1994 and (*b*) 1994/1995 (source: EEI, see figure 1 for locations).

2.3 *NDVI data*

NDVI time series from 1993 to 1995 were available from measurements of the Advanced Very High Resolution Radiometer (AVHRR) on board National Oceanic and Atmospheric Administration (NOAA) satellites only. This sensor has served as a continuous recording device for more than two decades now and has been widely used for vegetation studies (e.g. Ehrlich *et al.* 1994, Sannier *et al.* 2002, Al-Bakri and Taylor 2003). With a coarse spatial resolution of 1.1 km × 1.1 km at nadir, the AVHRR provides daily global coverage and allows creation of least cloud contaminated images for ample regions by producing temporal composites (Holben 1986, Cihlar *et al.* 1991).

Daily images of the AVHRR in High Resolution Picture Transmission (HRPT) format have been captured at a local receiving station in Etosha since 1993. After data broadcast, a pre-processing routine is applied at EEI (Le Roux 2002), which includes geometric correction and at-satellite reflectance conversion by using time-dependent coefficients. The coefficients account for platform differences, orbit-drift and sensor degradation of the AVHRR (Goward *et al.* 1991, Gutman 1991). After an additional cloud screening, 10-day Maximum Value Composites (MVC) of NDVI were produced to get least cloud contaminated images (Holben 1986, Le

Roux 2002). Readily processed MVCs were provided by EEI for this study comprising the time span from July 1993 to June 1995.

From visual inspection we discovered that during the rainy season the 10-day compositing interval is too short to get cloud-free images. As cloudy pixels were masked during the cloud screening (Le Roux 2002 unpublished report), data gaps occurred in the time series. To prevent these pixels from influencing data analysis and interpretation, gaps were filled by applying simple linear temporal interpolation as described in Eiden (2000).

2.4 *Fourier analysis*

In a closed interval [0; L], each continuous and periodic function $f(t)$ can be decomposed into a series of sine-waves with increasing frequency (Schönwiese 2000). This method is termed Fourier analysis and has been modified to be applicable to discrete time-series data, like the NDVI of a given pixel (see Jakubauskas *et al.* 2001 for a detailed description):

$$f(t)=\overline{f(t)}+\sum_{n=1}^{L/2}\left(A_n\cos\frac{2\pi nt}{L}-\phi_n\right) \tag{2}$$

Where $f(t)$ is the NDVI of a given pixel location at time t (1 year=36 ten-day MVCs, t=[1..36]); $\overline{f(t)}$ is the mean of $f(t)$ in [0; L], additive term; n is the harmonic term; A_n is the amplitude of the nth harmonic; ϕ_n is the phase angle of the nth harmonic; and L is the length of the observation period (L=36).

As mentioned above, Fourier analysis has turned out to be a suitable technique for parameterization of NDVI time series for several reasons (Azzali and Menenti 2000, Jakubauskas *et al.* 2001, Moody and Johnson 2001). At first, non-periodic and infrequent radiometric noise (e.g. from atmospheric attenuation, preprocessing errors) is restricted to higher terms. Thus, Fourier analysis is an effective smoothing procedure. Additionally, parameters of lower Fourier terms can be interpreted in terms of vegetation growth patterns. This holds for the mean, which is a good measure of overall greenness for a given pixel location. Furthermore, amplitude values quantify the degree of seasonal biomass production, whereas the number of the corresponding term is related to the amount of peaks during the observation period. The phase angle describes the time lag between origin and peak and captures the date of maximum greenness.

Admittedly, there are also some drawbacks of this method, which need to be mentioned as well. The underlying assumption of Fourier analysis is a periodical and sinusoidal signal, which is not strictly satisfied by the NDVI of a certain location. In fact, vegetation development related to actual growth conditions usually results in a complex shape of NDVI, which is not necessarily sinusoidal and requires higher frequency terms for suitable approximation. Although these higher terms might sometimes be related to growth patterns of secondary cover types as suggested by Moody and Johnson (2001), their meaning is commonly not straightforward. Thus, interpretation within this paper in relation to vegetation growth is mainly restricted to mean and first term parameters.

Fourier analysis was applied on a per-pixel basis separately for both periods (each from July to June), to capture vegetation growth in both seasons. The poor periodicity of NDVI is therefore irrelevant within this application. In accordance with previous work, images of mean [NDVI], amplitude [NDVI] and phase [month] of the first three terms were computed (Eiden 2000, Jakubauskas *et al.* 2001, Moody and Johnson 2001). Furthermore, the ratio of variance explained was derived for each of these terms to evaluate the degrees of information content (Schönwiese 2000). For all images, stratification was performed based on the reference map in order to compare NDVI specifications between vegetation entities and both periods.

3. Results

3.1 *Vegetation growth in ENP for 1993/1994 and 1994/1995*

Images of variance and Fourier parameters (mean, amplitude, phase) are shown in figure 4 with corresponding image statistics in tables 1 and 2. These data facilitate a comparative description of vegetation growth in ENP for both rainy seasons.

Variance image statistics suggest unimodal behaviour of NDVI and vegetation growth, respectively in both seasons, as across the area high percentages of data variation are captured by the first Fourier term (table 1). This is obviously related to the rainfall conditions with one seasonal maximum (Jakubauskas *et al.* 2001, figure 2). Despite the noisy appearance in figure 4((*a*) and (*b*)), spatial patterns of first-term variance differ significantly for both seasons as do contributions from higher Fourier terms. This clearly illustrates that NDVI trajectories do not show sinusoidal and periodical behaviour during the two seasons. Instead, vegetation growth seems to vary substantially across space and time.

At first, average greenness expressed as seasonal mean is clearly higher in 1993/1994 than in 1994/1995 (table 2, figure 4(*c*) and (*d*)). This holds for the entire park, but is most accentuated in the tree savannah regions of the eastern and northern part. Low greenness characterizes the Etosha pan and its eastern edge, which are either bare soil or covered by grassland and steppe formations with comparably low photosynthetic activity. In addition, amplitude and phase statistics and spatial patterns indicate large differences in amount and timing of seasonal productivity (figure 4(*e*)–(*h*)). Again, in 1993/1994 tree savannah is the most productive plant formation showing regional maxima of first-order amplitudes, whereas productivity is significantly reduced in 1994/1995. Biomass production decreases to moderate amounts for shrub savannah in the west and is constantly low for grassland and bare soil. Phase angles ranging from 0 (=July) to 2π (=June) suggest a peak of vegetation greenness around January/February nearly everywhere in the study area during 1993/1994. Contrariwise, a delayed culmination is indicated for 1994/1995, as maximum NDVI occurs in March and April (figure 4(*g*) and (*h*)).

The few rainfall records suggest that the east of ENP (Namutoni) receives appreciable amounts of precipitation throughout the season 1993/1994, whereas rainfall is less profitable towards the central (Okaukuejo) and western (Otjovasandu) parts. Accordance with the observed patterns of vegetation greenness and productivity is obvious. Apparently, during 1994/1995 rainfall is higher in the west and, in general, less evenly distributed throughout the season with almost no precipitation until February. Assuming a lagged response of vegetation growth to water availability is reasonable and explains the remarkable delay in culmination for 1994/1995.

3.2 *Parameter variations within and across vegetation entities*

Obviously, vegetation growth differs largely in terms of overall greenness, biomass production and date of maximum greenness for both seasons. However, as discussed

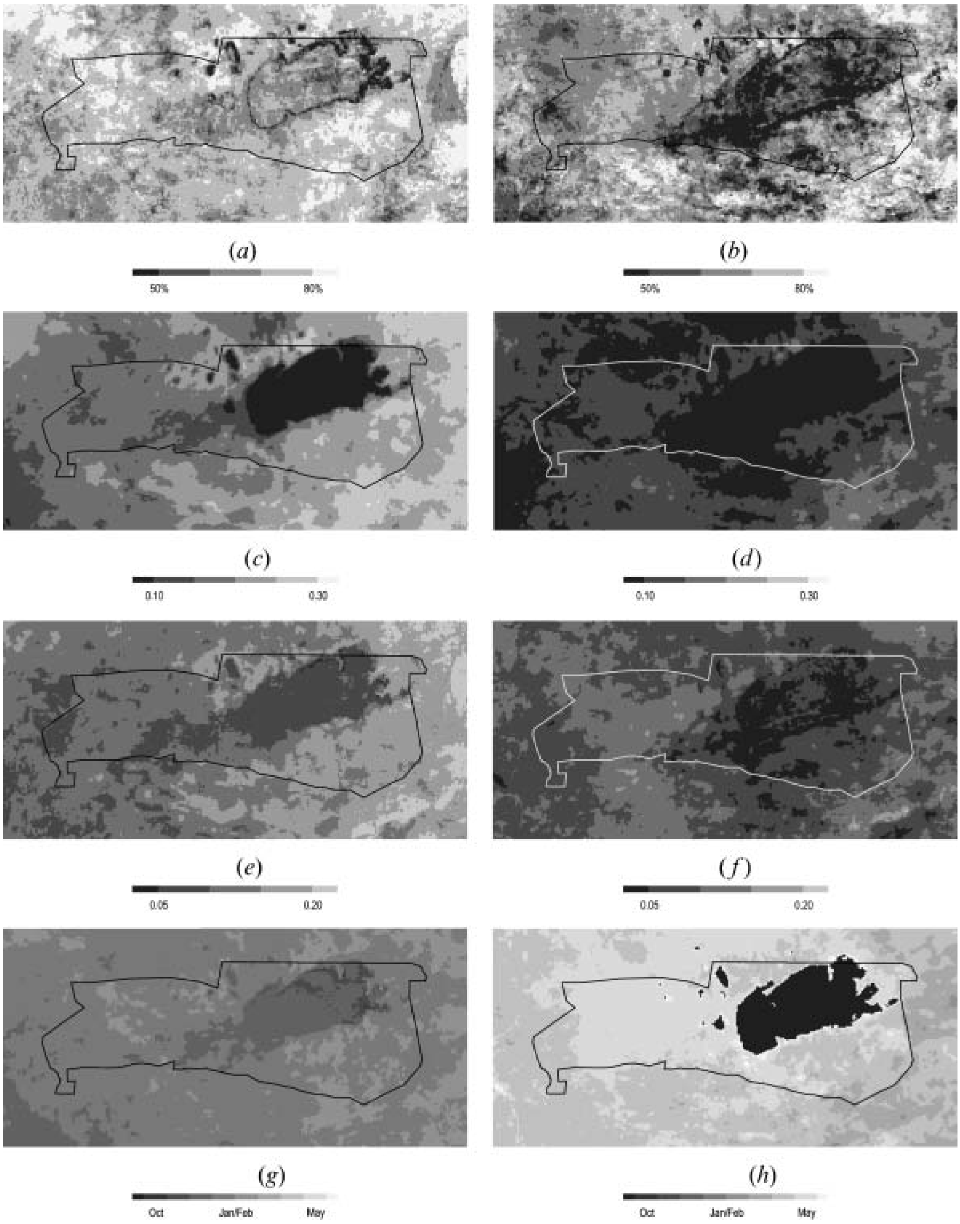

Figure 4. Images of variance, mean, first term amplitude and phase. Percentage variance explained by term 1 (*a*) 1993/1994, (*b*) 1994/1995. Seasonal mean for (*c*) 1993/1994 (NDVI), (*d*) 1994/1995 (NDVI). Amplitude of term 1 for (*e*) 1993/1994 (NDVI), (*f*) 1994/1995 (NDVI). Phase of term 1 for (*g*) 1993/1994, (*h*) 1994/1995.

earlier, evidence exists suggesting vegetation formations to be distinguishable by phenological patterns. Hence, it remains to be answered, if differences in NDVI and derived Fourier parameters between vegetation entities are exceeded by temporal variations in vegetation growth caused by variable rainfall conditions. To cope with this question, temporal NDVI signatures for all reference map units and both periods are shown in figure 6 (NDVI and Fourier representation from terms 0..3).

Table 1. Descriptive statistics of variance images.

Variance explained	Season 1993/1994		Season 1994/1995	
	Image mean	Image SD	Image mean	Image SD
Term 1	0.73	0.08	0.65	0.12
Term 2	0.1	0.04	0.13	0.07
Term 3	0.03	0.02	0.1	0.05
Sum	0.86		0.79	

Image values of mean and first-term amplitude/phase were further stratified for the four classes and visualized statistically using Box-Whisker plots (figure 5). The box sizes display the spatial average of a given Fourier parameter ± one standard deviation and thus, demonstrate within-class scattering.

For a given season, vegetation greenness (or mean NDVI) rises continuously from bare soil to tree savannah (figure 5(*a*)). However, distinction between grassland and shrub savannah as well as between shrub savannah and tree savannah is low in both periods, due to significant within-class variation. Lower vegetation greenness during 1994/1995 was noticed earlier and is once more highlighted in the box-plots. Remarkably, mean NDVI even differs for bare soil with vegetation cover either being very low or absent. Especially, the negative values in 1994/1995 can be ascribed to the Etosha pan, which makes up most of this unit and is occasionally covered by standing water after excessive rainfall events. Clearly, inter-seasonal variations outrange inter-class variations, which are additionally weakened by within-class scattering, e.g. mean NDVI of bare soil in 1993/1994 is close to grassland in 1994/1995, and grassland greenness in 1993/1994 even exceeds that of shrub and tree savannah in 1994/1995.

Within-class scattering is even enhanced for seasonal biomass production expressed as first-term amplitude values (figure 5(*b*)). Though class means show a slight increase from bare soil to tree savannah in 1993/1994, the productivity of shrub savannah partially exceeded tree savannah in 1994/1995. These findings are further supported by the temporal shapes of Fourier NDVI in figure 6((*c*) and (*d*)). For this parameter again, changes related to vegetation categories are widely exceeded by intra-class and inter-seasonal fluctuations.

Scatter is very low generally for first-term phase angles during 1993/1994 (figure 5(*c*)), though separability between plant formations is also weak with maximum greenness occurring everywhere around January. Trajectories in figure 6((*a*)–(*d*)) illustrate the similar culmination of NDVI. For bare soil, phase

Table 2. Descriptive statistics of Fourier parameters.

Fourier Parameters	Season 1993/1994		Season 1994/1995	
	Image mean	Image SD	Image mean	Image SD
Seasonal mean (NDVI)	0.19	0.06	0.10	0.06
Amplitude term 1	0.13	0.04	0.09	0.03
Amplitude term 2	0.05	0.02	0.04	0.02
Amplitude term 3	0.02	0.01	0.03	0.01
Phase term 1 (0; 2π)	3.42	0.28	4.78	1.24
Phase term 2 (0; 2π)	0.89	1.21	3.36	0.8
Phase term 3 (0; 2π)	1.86	1.49	2.37	0.45

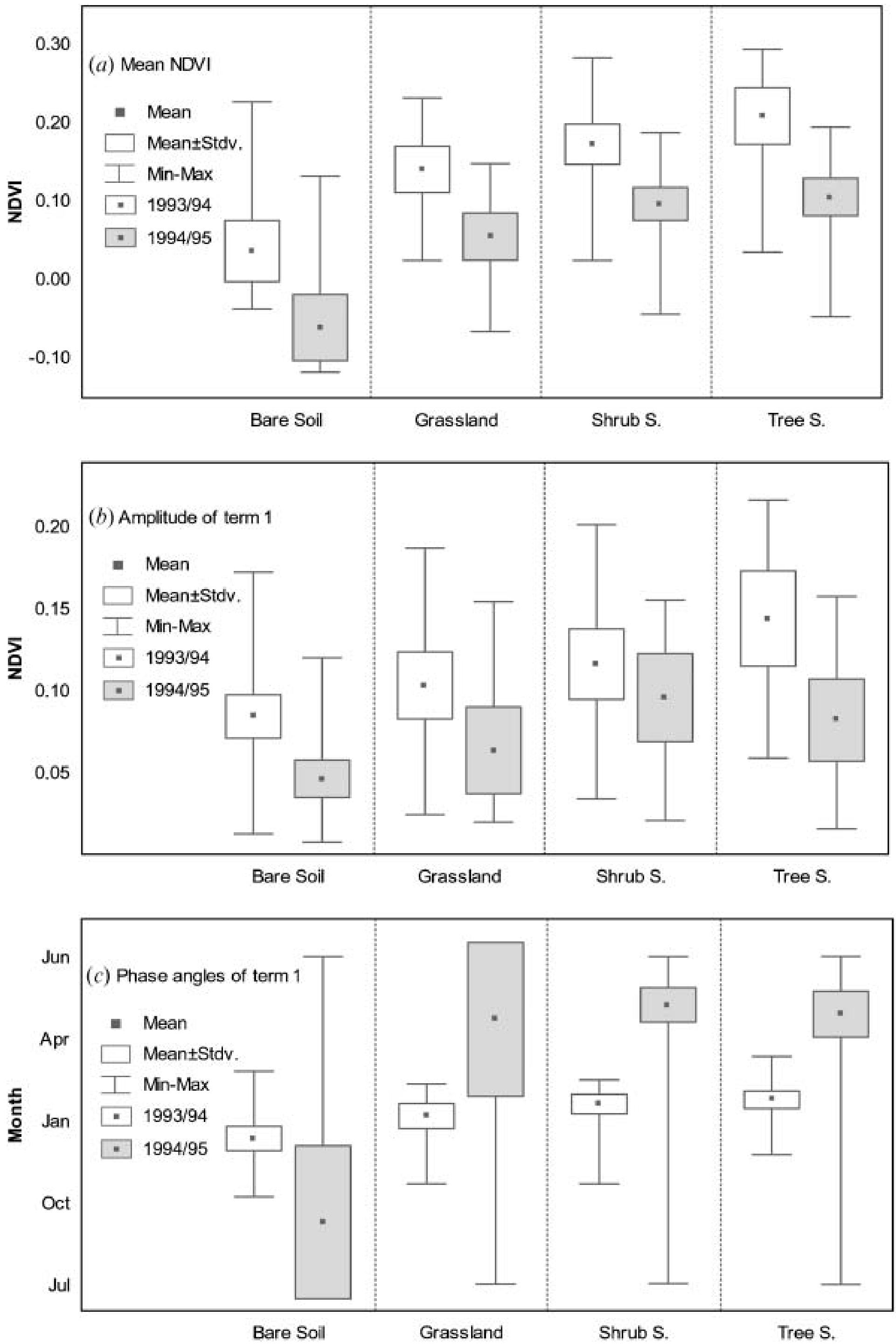

Figure 5. Box-Whisker plots of (*a*) mean, (*b*) first term amplitude and (*c*) first term phase, stratified for map units bare soil, grassland, shrub and tree savannah.

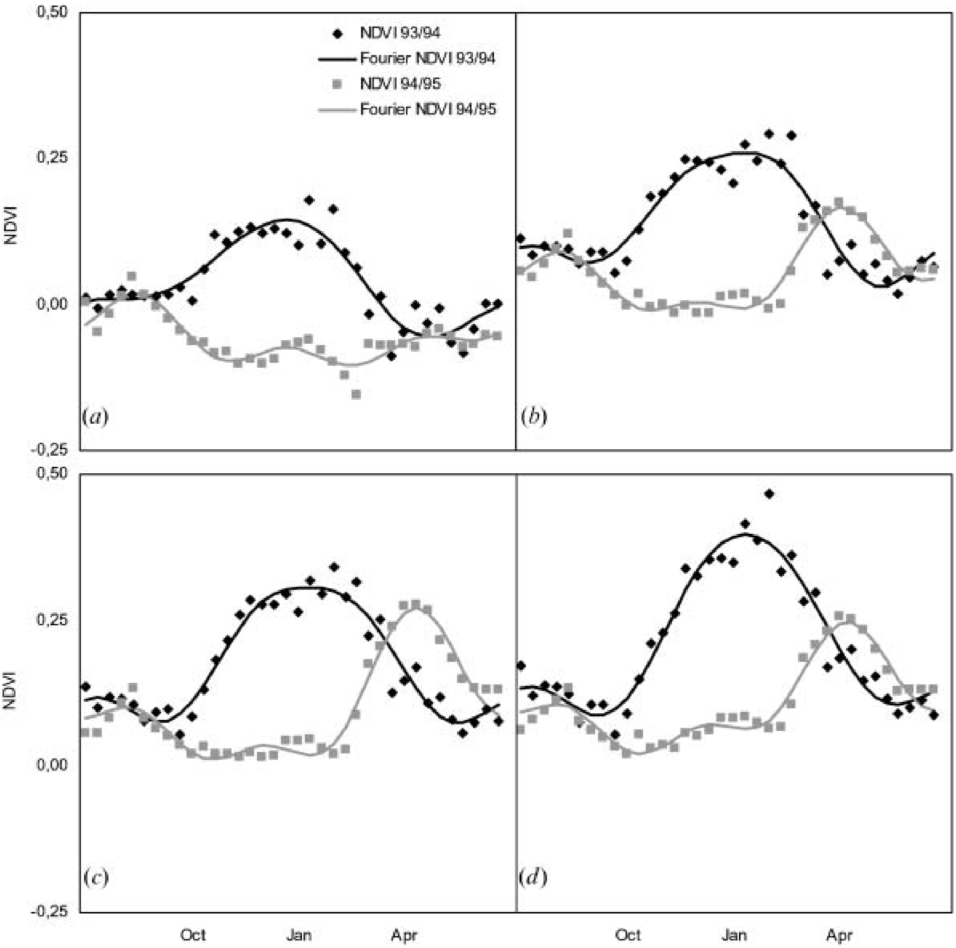

Figure 6. NDVI and Fourier NDVI stratified for map units (*a*) bare soil, (*b*) grassland/steppe, (*c*) shrub savannah and (*d*) tree savannah.

angles in 1994/1995 vary a good deal and suggest NDVI peaking between July and October, which is obviously unrelated to the rainy season (figure 6(*a*)). In combination with the negative temporal mean this proves that standing water probably controls NDVI behaviour for this land-cover class. For grassland, within-class scatter is ample too, and proposes maximum greenness between February and June. The same applies to shrub and tree savannah, but with more uniform class behaviour (figure 6(*b*)–(*d*)).

3.3 *Parameter-based image classifications*

Separability of vegetation formations based on individual NDVI-derived Fourier parameters is weak within a given season due to significant intra-class variations. Additionally, differences in vegetation growth are even more pronounced inter-seasonally.

Discrimination of cover types was finally tested by combining the available parameters in a clustering procedure. Partitioning was performed using the Iterative

Self-Organizing Data Analysis Technique (ISODATA), as suggested by Azzali and Menenti (2000) and Moody and Johnson (2001). Variance statistics (table 1) were used to select terms with significant information content independent of the results above. We assume that in 1993/1994 all Fourier parameters up to the second term contain important information (cumulative variance: 83%, figure 7(*a*)), and additionally the third term has to be included in 1994/1995 (cumulative variance: 88%, figure 7(*b*)). Using these parameters as classification variables, initially 20 classes were computed and merged afterwards based on Euclidean distances to four major categories in accordance with the reference map. Misclassifications were analysed using confusion matrices, which are commonly generated by a cross-tabulation of frequency of occurrence for all possible class combinations between result and reference (Taylor *et al.* 1996).

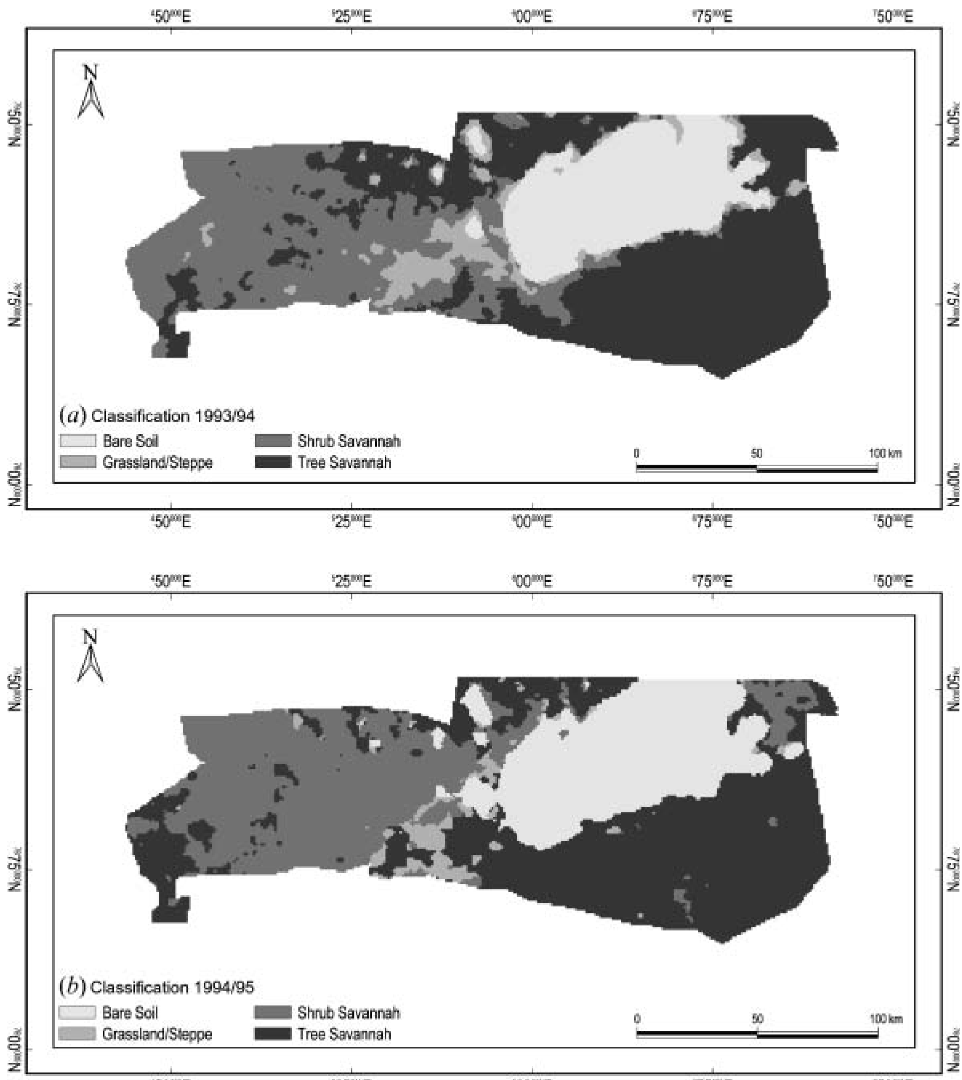

Figure 7. Classifications of Fourier parameters for (*a*) 1993/1994 (terms 1–2) and (*b*) 1994/1995 (terms 1–3).

Overall agreement between our (Fourier) classifications and the vegetation map is 74.51% for 1993/1994 and 72.13% for 1994/1995 (table 3(*a*) and (*b*)). Best results were gained for bare soil in both seasons with accuracies close to or even above 90%. For tree savannah, separability is also reasonable. However, confusion with shrub savannah and vice versa is obvious. Large misclassifications can be detected for grassland. For example, only 18% were detected correctly by the Fourier classification in 1994/1995 and large proportions from other units are usually included in this class (e.g. soil in 1993/1994, shrub savannah in 1994/1995).

An intersection of the two Fourier classifications and the vegetation map was produced to identify areas that have been attributed properly in both seasons (figure 8). Detection of bare soil seems to be largely season independent, which is not an amazing result, as the Etosha pan is a very obvious feature within the study area making up most of this class. Tree savannah in the south-eastern part of ENP is well captured in accordance with the vegetation map, resulting in 64% of this unit being classified properly. A heterogeneous patchwork of shrubs and trees is found in large areas of the central north and in the south-western corner resulting in inter-seasonal confusion of both units during the classification process. Nevertheless, 55% of shrub savannah was still captured by NDVI behaviour in both years. Least inter-seasonal agreement is found for grassland/steppe. This vegetation unit seems to be most influenced by inter-seasonal variations in growth conditions.

Table 3. Consistency between parameter classification and reference map.

(*a*) 1993/1994

	Vegetation map					
Classification	Bare soil	Grassland/ steppe	Shrub savannah	Tree savannah	Total	Accuracy (%)
Bare soil	4515	44	8	6	4573	98.73
Grassland/ steppe	436	742	214	209	1601	46.35
Shrub savannah	86	856	4536	2218	7696	58.94
Tree savannah	68	171	1841	8207	10287	79.78
Total	5105	1813	6599	10640	24157	
Accuracy (%)	88.44	40.93	68.74	77.13		

Overall accuracy: 74.51%, Kappa: 0.63

(*b*) 1994/1995

	Vegetation map					
Classification	Bare soil	Grassland/ steppe	Shrub savannah	Tree savannah	Total	Accuracy (%)
Bare soil	4925	370	35	91	5421	90.85
Grassland/ steppe	14	323	319	154	810	39.88
Shrub savannah	66	395	4460	2679	7600	58.68
Tree savannah	100	725	1785	7716	10326	74.72
Total	5105	1813	6599	10640	24157	
Accuracy (%)	96.47	17.82	67.59	72.52		

Overall accuracy: 72.13%, Kappa: 0.59

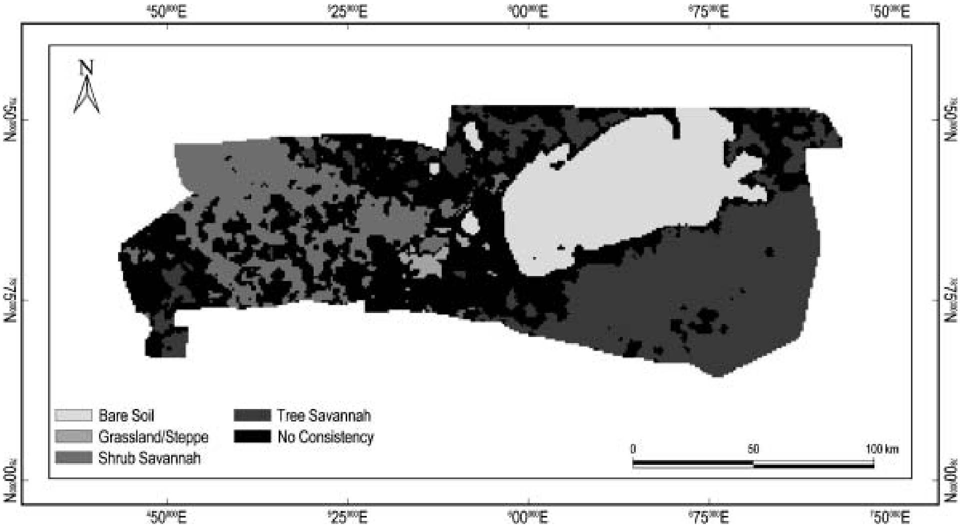

Figure 8. Consistency between the Fourier classifications of 1993/1994 and 1994/1995 and the Etosha vegetation map.

4. Discussion and conclusion

Usability of Fourier analysis for NDVI time series parameterization is well documented in the literature (Jakubauskas *et al.* 2001, Moody and Johnson 2001) and is confirmed by our analysis. Already the first term accounts for the majority of data variance and the parameter mean, amplitude and phase can be well interpreted in relation to vegetation phenology. Hence, this method outperforms other ways of data reduction such as principal component analysis (PCA, see Eastman and Fulk 1993), where interpretation is difficult or even impossible.

However, vegetation formations only differed slightly intra-seasonally in terms of vegetation greenness, productivity and peaking date due to intensive within-class scattering. Obviously, plant growth is controlled by local rainfall causing different phenologies and thus, different Fourier parameters even within a given formation due to spatial precipitation variability. These spatial variations are even exceeded in the temporal domain. Within our narrow timeframe of only two periods, inter-seasonal fluctuations were largest above all and exceeded intra-class and inter-class variations. As rainfall variability in dry savannahs such as ENP is very high, the results are very likely to be the same when comparing data from multiple seasons.

Considerable agreement between both classifications and the reference map is supported by overall accuracies around 70% and Kappa coefficients of 0.59 and 0.63 (Lillesand and Kiefer 2000). However, as only four major vegetation categories were considered, this is only a moderate value and not a satisfying result. A further decrease in accuracy can be assumed if more different vegetation units are examined. Nevertheless, the degree of correspondence is also limited by the quality of the reference map. As this was determined to be 89% correct, even a 100% correct Fourier map would only agree by 89% (Moody and Johnson 2001).

At least partially the results may be ascribed to NDVI data quality and the chosen methodology. At first, AVHRR data are known to suffer from orbit drift resulting in changes in illumination conditions and sensor degradation (Goward *et al.* 1991, Gutman 1991). Although methods exist to correct data for these errors (Los 1993, Roderick *et al.* 1996), readily processed NDVI data from EEI were the only data source for this study (Le Roux 2002) and thus, data accuracy remains questionable. Additionally, Fourier parameters quantify only certain aspects of vegetation phenology. Separability among cover types might be improved by other metrics such as growth duration or dry season minimum. So it remains to be investigated, if the results can be improved by using data from reliable sources and/or advanced sensors (MODIS, Vegetation) in combination with different phenological metrics and up-to-date reference datasets.

Acknowledgment

This research project was funded by the German Research Foundation (Deutsche Forschungsgemeinschaft) under contracts SA 775/3-1 and SA 775/5-1. Satellite and reference data were provided by Johan Le Roux, EEI. Professor Dr Donald Friend, Dr Henning Schröder and Dr Jan Richters provided many useful comments on the manuscript.

References

AL-BAKRI, J. and TAYLOR, J., 2003, Application of NOAA AVHRR for monitoring vegetation conditions and biomass in Jordan. *Journal of Arid Environments*, **54**, pp. 579–593.

AZZALI, S. and MENENTI, M., 2000, Mapping vegetation-soil-climate complexes in Southern Africa using temporal Fourier analysis of NOAA-AVHRR NDVI data. *International Journal of Remote Sensing*, **21**, pp. 973–996.

BEUGLER-BELL, H., 1996, Öko-pedologische Untersuchungen im Etoscha Nationalpark und angrenzenden Landschaften in Nordnamibia unter besonderer Berücksichtigung der Bodenerosion als limitierender Faktor einer nachhaltigen Bewirtschaftung semiarider Savannenökosysteme. PhD thesis, Institute of Geography, University of Regensburg, Germany.

CARLSON, T. and RIPLEY, D., 1997, On the relation between NDVI, fractional vegetation cover, and Leaf Area Index. *Remote Sensing of Environment*, **62**, pp. 241–252.

CIHLAR, J., ST.-LAURENT, L. and DYER, J., 1991, Relation between the Normalized Difference Vegetation Index and ecological variables. *Remote Sensing of Environment*, **35**, pp. 279–298.

DAVENPORT, M. and NICHOLSON, S., 1993, On the relationship between rainfall and the Normalized Difference Vegetation Index for diverse vegetation types in East Africa. *International Journal of Remote Sensing*, **14**, pp. 2369–2389.

DEFRIES, R., HANSEN, M. and TOWNSHEND, J., 1995, Global discrimination of land cover types from metrics derived from AVHRR Pathfinder data. *Remote Sensing of Environment*, **54**, pp. 209–222.

DIALLO, O., DIOUF, A., HANAN, N., NDIAYE, A. and PRÉVOST, Y., 1991, AVHRR monitoring of savanna primary production in Senegal, West Africa: 1987–1988. *International Journal of Remote Sensing*, **12**, pp. 1259–1279.

DIOUF, A. and LAMBIN, E., 2001, Monitoring land-cover changes in semi-arid regions: remote sensing data and field observations in the Ferlo, Senegal. *Journal of Arid Environments*, **48**, pp. 129–148.

DU PLESSIS, W., 1999, Linear regression relationships between NDVI, vegetation and rainfall in Etosha National Park, Namibia. *Journal of Arid Environments*, **42**, pp. 235–260.

EASTMAN, J. and FULK, M., 1993, Long sequence time series evaluation using standardized principal components. *Photogrammetric Engineering and Remote Sensing*, **59**, pp. 1307–1312.

EHRLICH, D., ESTES, J. and SINGH, A., 1994, Applications of NOAA-AVHRR 1 km data for environmental monitoring. *International Journal of Remote Sensing*, **15**, pp. 145–161.

EIDEN, G., 2000, *Charakterisierung der raum-zeitlichen Vegetationsdynamik von dürre- und desertifikationsgefährdeten, ariden und semi-ariden Regionen. Materialien Zur Ostafrika-Forschung* (Germany: Selbstver lag der Geographischen Gesellschaft Trier).

GOWARD, S., MARKHAM, B., DYE, D., DULANEY, W. and YANG, J., 1991, Normalized Difference Vegetation Index measurements from the Advanced Very High Resolution Radiometer. *Remote Sensing of Environment*, **35**, pp. 257–277.

GUTMAN, G., 1991, Vegetation indices from AVHRR: an update and future prospects. *Remote Sensing of Environment*, **35**, pp. 121–136.

HIGGINS, S., SHACKLETON, C. and ROBINSON, E., 1999, Changes in woody community structure and composition under constrasting landuse systems in a semi-arid savanna, South Africa. *Journal of Biogeography*, **26**, pp. 619–627.

HOLBEN, B., 1986, Characteristics of maximum-value composite images from temporal AVHRR data. *International Journal of Remote Sensing*, **7**, pp. 1417–1434.

JAKUBAUSKAS, M., LEGATES, D. and KASTENS, J., 2001, Harmonic analysis of time-series AVHRR NDVI data. *Photogrammetric Engineering and Remote Sensing*, **67**, pp. 461–470.

JUSTICE, C. and HIERNAUX, P., 1986, Monitoring grasslands of the Sahel using NOAA AVHRR data: Niger 1983. *International Journal of Remote Sensing*, **7**, pp. 1475–1497.

JUSTICE, C., HOLBEN, B. and GWYNNE, M., 1986, Monitoring East African vegetation using AVHRR data. *International Journal of Remote Sensing*, **7**, pp. 1453–1474.

KREMER, R. and RUNNING, S., 1993, Community type differentiation using NOAA/AVHRR data within a sagebrush-steppe ecosystem. *Remote Sensing of Environment*, **46**, pp. 311–318.

LE ROUX, J., 2002, Satellite image capture and pre-processing at the Etosha Ecological Institute. Ministery of Environment and Tourism, Namibia, unpublished report.

LE ROUX, C., GRUNOW, J., MORRIS, J., BREDENKAMP, G. and SCHEEPERS, J., 1988, A classification of the vegetation of the Etosha National Park. *South African Journal of Botany*, **54**, pp. 1–10.

LI, J., LEWIS, J., ROWLAND, J., TAPPAN, G. and TIESZEN, L., 2004, Evaluation of land performance in Senegal using multi-temporal NDVI and rainfall series. *Journal of Arid Environments*, **59**, pp. 463–480.

LILLESAND, T. and KIEFER, R., 2000, *Remote Sensing and Image Interpretation* (New York: John Wiley & Sons).

LOS, S., 1993, Calibration adjustment of the NOAA AVHRR Normalized Difference Vegetation Index without recourse to component channel 1 and 2 data. *International Journal of Remote Sensing*, **14**, pp. 1907–1917.

MALINGREAU, J., TUCKER, C. and LAPORTE, N., 1989, AVHRR for monitoring global tropical deforestation. *International Journal of Remote Sensing*, **10**, pp. 855–867.

MENDELSOHN, J., JARVIS, A., ROBERTS, C. and ROBERTSON, T., 2002, *Atlas of Namibia* (Cape Town: The Ministry of Environment and Tourism of Namibia).

MOODY, A. and JOHNSON, D., 2001, Land-surface phenologies from AVHRR using the discrete Fourier transform. *Remote Sensing of Environment*, **75**, pp. 305–323.

MOULIN, S., KERGOAT, L., VIOVY, N. and DEDIEU, G., 1997, Global-scale assessment of vegetation phenology using NOAA/AVHRR satellite measurements. *Journal of Climate*, **10**, pp. 1154–1170.

NICHOLSON, S. and FARRAR, T., 1994, The influence of soil type on the relationships between NDVI, rainfall, and soil moisture in semiarid Botswana. I. NDVI response to rainfall. *Remote Sensing of Environment*, **50**, pp. 107–120.

PICKUP, G. and CHEWINGS, V., 1994, A grazing gradient approach to land degradation assessment in arid areas from remotely-sensed data. *International Journal of Remote Sensing*, **15**, pp. 597–617.

PRINCE, S., 1991, Satellite remote sensing of primary production: comparison of results for Sahelian grasslands 1981–1988. *International Journal of Remote Sensing*, **12**, pp. 1301–1311.

REED, B., BROWN, J., VANDERZEE, D., LOVELAND, T., MERCHANT, J. and OHLEN, D., 1994, Measuring phenological variability from satellite imagery. *Journal of Vegetation Science*, **5**, pp. 703–714.

RICHARD, Y. and POCCARD, I., 1998, A statistical study of NDVI sensitivity to seasonal and interannual rainfall variations in Southern Africa. *International Journal of Remote Sensing*, **19**, pp. 2907–2920.

RODERICK, M., SMITH, R. and LODWICK, G., 1996, Calibrating long-term AVHRR-derived NDVI imagery. *Remote Sensing of Environment*, **58**, pp. 1–12.

ROQUES, K., O'CONNOR, T. and WATKINSON, A., 2001, Dynamics of shrub encroachment in an African savanna: relative influences of fire, herbivory, rainfall and density dependence. *Journal of Applied Ecology*, **38**, pp. 268–280.

SANNIER, C., TAYLOR, J., DU PLESSIS, W. and CAMPBELL, K., 1996, Application of remote sensing and GIS for monitoring vegetation in Etosha National Park. In *Remote Sensing and GIS for Natural Resource Management*, L. Rosenberg, C. Power and I. Downey (Eds), pp. 101–106 (Chatham: Natural Resources Institute).

SANNIER, C., TAYLOR, J. and DU PLESSIS, W., 2002, Real-time monitoring of vegetation biomass with NOAA-AVHRR in Etosha National Park, Namibia, for fire risk assessment. *International Journal of Remote Sensing*, **23**, pp. 71–89.

SCHOLES, R. and WALKER, B., 1993, *An African Savanna: Synthesis of the Nylsvley study* (Cambridge: Cambridge University Press).

SCHÖNWIESE, C., 2000, *Praktische Statistik für Meteorologen und Geowissenschaftler*, 3rd edn (Berlin: Gebrüder Borntraeger).

SCHULTZ, J., 2000, *Handbuch der Ökozonen* (Stuttgart: Ulmer).

TAYLOR, J., BIRD, A., SANNIER, C., PRATT, N. and DU PLESSIS, W., 1996, Calibration and validation of thematic maps from remote sensing in developing countries: need and method. In *Remote Sensing and GIS for Natural Resource Management*, L. Rosenberg, C. Power and I. Downey (Eds), pp. 39–46 (Chatham: Natural Resources Institute).

WORLD BANK GROUP, 2004, Terrafrica: Halting land degradation. Available online at: http://web.worldbank.org/WBSITE/EXTERNAL/NEWS/0,,contentMDK:20221507~menuPK:34457~pagePK:64003015~piPK:64003012~theSitePK:4607,00.html# (accessed 2 July 2004).

XIAO, J. and MOODY, A., 2004, Photosynthetic activity of US biomes: response to the spatial variability and seasonality of precipitation and temperature. *Global Change Biology*, **10**, pp. 437–451.